Soil & Tillage Research 110 (2010) 77–86

Contents lists available at ScienceDirect

Soil & Tillage Research

journal homepage: www.elsevier.com/locate/still

Spatial complexity of soil plow layer penetrometer resistance as influenced by sugarcane harvesting: A prefractal approach

Luís D. Pérez [a], Humberto Millán [b,*], Mario González-Posada [b]

[a] Department of Agricultural Engineering, University of Granma, Apdo. 21, Bayamo 85100, Granma, Cuba
[b] Department of Physics and Chemistry, University of Granma, Apdo. 21, Bayamo 85100, Granma, Cuba

ARTICLE INFO

Article history:
Received 10 February 2010
Received in revised form 22 June 2010
Accepted 24 June 2010

Keywords:
Soil compaction
Sugarcane
Geostatistics
Prefractal analysis

ABSTRACT

Sugarcane is one important crop for many Third World countries. Soils dedicated to sugarcane are usually compacted during the harvesting process. The main objective of the present work was to search for prefractal scaling patterns of soil compaction before and after sugarcane harvest. We used descriptive statistics and prefractal analysis with experimental semivariograms for characterizing the spatial patterns of soil penetrometer resistance distributions. The soil is a Vertisol (Typic Hapludert) dedicated to sugarcane production during the last 60 years. Approximately 50% of soil resistance values were over 2.5 MPa after sugarcane harvest. This could restrict sugarcane shoot emergence. A power-law (prefractal) model fitted experimental semivariograms fairly well except for those distributions corresponding to 2.5–5.0 cm soil depth. Those particular distributions could be fitted by any standard geostatistical model. The main findings were (i) scaling exponents larger than 1.5 which indicate anti-persistence and (ii) change of anisotropic directions after sugarcane harvest. The range of prefractal behaviour was approximately 105 m before harvest and 93 m after crop harvest. The spatial structure of some soil physical or mechanical properties connected to soil compaction can resemble those patterns. The combination of Geostatistics and prefractal analysis can assist the mechanized agriculture and scientists through a previous identification of degraded zones within the field and the physical processes involved in the formation of those local areas.

© 2010 Elsevier B.V. All rights reserved.

1. Introduction

Sugarcane is still the main plantation crop for the economy of many developing countries located in tropical regions (e.g. African and Caribbean areas) while some developed countries (e.g. Australia and USA) also make important contributions to the global production of that crop. From an economical point of view, many industries around the world depend on sugarcane by-products (e.g. ethanol) (Sugarcane Production BMPs, 2000). Soils dedicated to sugarcane production are usually affected by multiple factors. Two important factors are monoculture and the use of heavy machinery for sugarcane harvesting (Hartemink, 1998). A direct effect of both aforementioned causes is the increase of soil compaction which limits rooting (Juang and Uehara, 1971). Soil compaction has reduced the production rate of sugarcane in Cuba approximately 21% since 1990 (unpublished report). That variable is usually estimated in terms of penetrometer resistance and its negative effect varies with crop type (Hadas, 1997). Some authors consider that root growth is null at a standard soil penetration resistance of about 5 MPa. For example, Materechera et al. (1991) set this limit to 5 MPa, Hadas (1997) reported a range from 1.6 MPa for corn to 3.7 MPa for barley while Duiker (2002) considered this extreme value as 2.06 MPa (300 psi). Regrettably, soil compaction is a cumulative process (Keller, 2004).

Applications of the Theory of Regionalized Variables (Geostatistics) and its multiple methods (Matheron, 1971) have signified important advances for quantifying spatial attributes of soil compaction at several observational scales. A main practical importance of the spatial variability analysis is associated with the opportunity of identifying degraded regions within the agricultural field. This can help scientists, engineers or farm managers to develop appropriate strategies of soil management (Webster and Burgess, 1980) and to develop site specific agricultural practices. Spatial variability analysis can also include, among others, soil texture, bulk density, pH, penetrometer resistance and water content as these soil properties can be affected considerably by soil compaction (Kiliç et al., 2000).

The combination of geostatistics and spatial fractal analysis has increased our toolbox for understanding soil spatial variability. Unfortunately most works combining geostatistics and fractal scaling have been conducted on unidirectional transects where the hypothesis of anisotropy could not be tested. In such cases one

* Corresponding author. Tel.: +53 23 427392.
E-mail address: hmillanv@udg.co.cu (H. Millán).

0167-1987/$ – see front matter © 2010 Elsevier B.V. All rights reserved.
doi:10.1016/j.still.2010.06.011

could be working with stationary or nonstationary processes but not necessarily isotropic. In general, this approach has been previously used by Armstrong (1986), Perfect et al. (1990) and Pan and Lu (1994) with soil penetrability data. In addition, Thomas and Thomas (1988) have considered the possibility of finding fractal dimensions depending on spatial orientation.

After harvesting a sugarcane field we can find two different scenarios: first of all an increase of soil resistance values at different depths of the field, and second, redistribution of soil compaction zones compared to those before sugarcane harvesting. If these behaviors can be quantified, then farmers could change their management practices to improve the productivity of sugarcane agriculture. Thus, our main hypothesis is based on the existence of anisotropic prefractal domains provided that semivariograms fit a Pareto-type model depending on spatial directions. The main objective of the present work was to search for prefractal scaling patterns of soil compaction before and after sugarcane harvest.

2. Theoretical considerations

Our main theoretical assumption considers that structure of spatial increments can be captured by a power-law relation (Korvin, 1992; Baveye et al., 2008):

$$|Z(r) - Z(r+h)| \propto h^H \tag{1}$$

where Z is the soil property value (e.g. penetrometer resistance) at the r spatial location, h is the lag distance (h is the absolute value of a distance vector) and H is the scaling exponent. Within the limits $0 < H < 1$, H is related to the Hausdorff-Besicovitch fractal dimension, D, by Webster (2008):

$$D = 2 - H \tag{2}$$

The semivariogram is usually defined as (Matheron, 1971):

$$\gamma(\vec{\mathbf{h}}) = \frac{1}{2}E[\{Z(\vec{\mathbf{r}}) - Z(\vec{\mathbf{r}} + \vec{\mathbf{h}})\}^2] = \mathrm{var}[Z(\vec{\mathbf{r}}) - Z(\vec{\mathbf{r}} + \vec{\mathbf{h}})] \tag{3}$$

where $\gamma(\vec{\mathbf{h}})$ is the semivariance and $[\{Z(\vec{\mathbf{r}}) - Z(\vec{\mathbf{r}} + \vec{\mathbf{h}})\}^2]$ is the expected value of $\{Z(\vec{\mathbf{r}}) - Z(\vec{\mathbf{r}} + \vec{\mathbf{h}})\}^2$.The semivariogram depends only on points separation and not on their absolute positions (Matheron, 1971). Eq. (3) represents the principal tool of geostatistics. Then, combining Eqs. (1)–(3):

$$\gamma(h) = \frac{1}{2}ch^{(4-2D_\nu)} \tag{4}$$

where c is a scaling coefficient accounting for the semivariogram behaviour as $h \to 0$ and D_ν is the fractal dimension of the semivariogram. Eq. (4) is usually called the structure function (Wu, 2000).

From a theoretical point of view, the exponent in Eq. (4) is determined as a limit, that is

$$4 - 2D_\nu \propto \lim_{h \to 0} \frac{\log \gamma(h)}{\log h} \tag{5}$$

From our standpoint, that is the main restriction of extrapolating theoretical results from fractal mathematics to experimental conditions. In practice, h is confined within lower and upper cutoffs, $h_{\min} < h < h_{\max}$, where $h_{\min} > 0$. Thus, following Perfect et al. (2002) rationale we use the term prefractal domain hereafter even though some authors (e.g. Krasilnikov, 2008) call it incomplete fractal behavior. Thus, the prefractal analysis allows one to quantify how the spatial pattern of the considered soil property (e.g. soil penetration resistance) evolves as the spatial scale (h value) changes. That spatial pattern is driven by its second order statistics (e.g. semivariance). This way, while the geostatistical analysis identifies affected zones within the field, prefractal analysis can shed light on the scaling mechanisms producing those areas.

Following Feder (1988) the correlation function of future increments with past increments (average increments) depends on H. Let us consider $-\Delta_H(-h)$ the increment at a previous lag, $-h$ (here the "$-$" sign indicates past with respect to a reference, $h = 0$) and $\Delta_H(+h)$ the corresponding increment at the next lag. Then the correlation function of upcoming increments, $\Delta_H(+h)$, with preceding increments, $-\Delta_H(-h)$ can be written as:

$$\frac{\langle -\Delta_H(-h)\Delta_H(+h)\rangle}{\langle \Delta_H(h)^2\rangle} = 2^{2H-1} - 1 \tag{6}$$

That is, the average spatial increment of the studied soil variable might be investigated in terms of a fractional Brownian motion. The left hand numerator in Eq. (6) states the probability of a future increment, $\Delta_H(+h)$, averaged over the distribution of past increments, $-\Delta_H(-h)$ (Feder, 1988; Molz et al., 1998).

Based on H values, some cases can be distinguished:

(i) $H = 1/2$ (or $D_\nu = 1.5$) has been identified with ordinary Brownian-like variations. In this case the correlation of successive increments vanishes as can be deduced from Eq. (6). This corresponds to Gauss–Markov processes.
(ii) The range $1/2 < H < 1$ ($1 < D_\nu < 1.5$) is usually associated with persistence (positive correlation), long-range spatial variation or clear trends (Feder, 1988). Physically, if the investigated soil property increases in average within a spatial lag h, it is statistically likely an increase within the next spatial lag. Thus, the statistics of persistence could be used for making predictions on the occurrence of extreme values of the considered variable.
(iii) The range $0 < H < 1/2$ ($1.5 < D_\nu < 2$) represents anti-persistent behavior (negative correlation) and short-range spatial variation. That is, the average spatial increment of the studied soil variable at a given spatial lag, h, is likely to be followed by a decrease within the next spatial domain. This short-range fluctuation pattern tends to the filling condition (e.g. $D_\nu \to 2$) such that it seems very noisy. That behavior indicates, to some extent, that other external or internal variables influence the variability of the analyzed property or process.

The presence of positive/negative correlations in the fluctuational dynamics of soil properties could be associated to the heterogeneous structure of soil system. In general, each H (D_ν) value needs to be interpreted within the context of each particular investigation. The power-law model as represented by Eq. (4) is valid for both isotropic and anisotropic analyses. Furthermore, that model (Eq. (4)) defines a statistically self-affine prefractal structure (Turcotte, 1997). That is, while self-similarity represents isotropy in relation to the observation scale, self-affine structures are usually associated with anisotropic patterns (Mandelbrot, 1986). Briefly, any two-dimensional function, $f(x, y)$, defining a self-affine spatial structure presents different scaling factors in different spatial directions (Baveye et al., 2008). In addition, there could be nested prefractal regimes separated by different crossover scales. This is also identified with self-affine structures (Mandelbrot, 1985).

Some authors have considered that significant fits of power-law (fractal) models to experimental semivariograms do not correspond necessarily to real prefractal structures (e.g. Burrough, 1989; McClean and Evans, 2000). Note however that validity of Eq. (4) with geostatistical data can violate (at least within the considered spatial scale) the second order statistics as the semivariance increases as a power-law function of the spatial

Fig. 1. Physical map of the studied area.

resolution (nonstationarity) with no sill in most cases. That behavior can occur within lower (sampling interval) and upper (plot size) scale cutoffs and justifies, to some extent, the use of prefractal models within those limits.

3. Materials and methods

3.1. Study site description

This study was conducted on a Vertisol (Typic Hapludert) (Soil Survey Staff, 2003) located in Bayamo, at south-eastern Cuba (20°22′N, 76°38′W) (Fig. 1). Table 1 shows some selected physical and chemical characteristics of the studied area. The site has been under sugarcane (*Saccharum officinarum* sp.) monoculture during the last 60 years which can produce yield decline due to soil properties degradation. Each sugarcane field represents a rectangle of approximately 4.5 ha (150 m width × 300 m long). Sugarcane is harvested in March each year using Case IH-Austoft series 7000 (Brazil) harvesters. Photographs (Fig. 2(a) and (b)) show the sugarcane field before harvest (first soil sampling) and approximately 15 days after crop harvest (second soil sampling), respectively.

3.2. Penetrometer resistance and soil property measurements

Soil resistance data were collected at the vertexes of regular squared grids. Before crop harvest we used a 12 × 12 = 144 points grid with sampling interval L = 10 m. After sugarcane harvest a 10 × 10 = 100 data points grid was considered with the same sampling distance. We were interested in inter-row points only (inter-row distance ≈ 1.9 m in the East direction) as inter-row is the main route of harvester wheels and accompanying trucks or tractors. It means that sampling points in the east direction were located every five inter-rows, approximately. In both cases we considered that a sample size between 100 and 150 data points was acceptable within the context of the present work. This also agrees with previous recommendations by Webster and Oliver (1992).

An electronic penetrometer (FIELDSCOUT™ SC900 Soil Compaction Meter, Spectrum Technologies, Inc., Illinois)[1] was used for soil resistance measurements. Some specific characteristics of this instrument are: in depth resolution = 2.5 cm, measurement resolution = 0.035 MPa, in depth range = 0–45 cm and cone index range = 0–7 MPa. Cone penetrometer readings were taken at four different depths from the plow layer before and after sugarcane harvest (0–2.5, 2.5–5.0, 5.0–7.5 and 7.5–10.0 cm).

[1] Trade name mention is only for scientific purpose, not for product endorsement.

Table 1
Some characteristics of the studied soil.

Soil characteristics	Mean	CV (%)
Clay (%)	51.90	3.32
Silt (%)	26.51	4.11
Sand (%)	21.59	2.56
pH (H_2O)	7.1	2.21
O.M. (%)	3.31	5.81

n = 15 soil samples in each case.

Fifteen disturbed soil samples were randomly collected (approximately 1 kg each one) within the first squared grid (120 m × 120 m grid). Fifteen sub-samples (approximately 50 g each sub-sample) were bagged in aluminium containers and weighted for soil moisture determinations (gravimetric method) after oven-drying at 105 °C. Each soil sample was extracted from the 0–10 cm soil depth using an auger. At the laboratory, undisturbed soil samples were air dried for 2 weeks, ground and passed through a 2.0 mm sieve. The pipette method (Gee and Bauder, 1986) was used for texture analysis, soil pH values were determined in H_2O using the potentiometric method (soil–solution ratio 2:5) and organic carbon (OC) by dry combustion (OM = 1.724 × OC). Soil moisture content was also determined after sugarcane harvest.

3.3. Standard statistics, prefractal and geostatistical analyses

Soil physical/chemical properties and penetrometer resistance data were characterized using standard descriptive statistics. In addition, Shapiro–Wilk tests of normality ($p < 0.05$ indicates

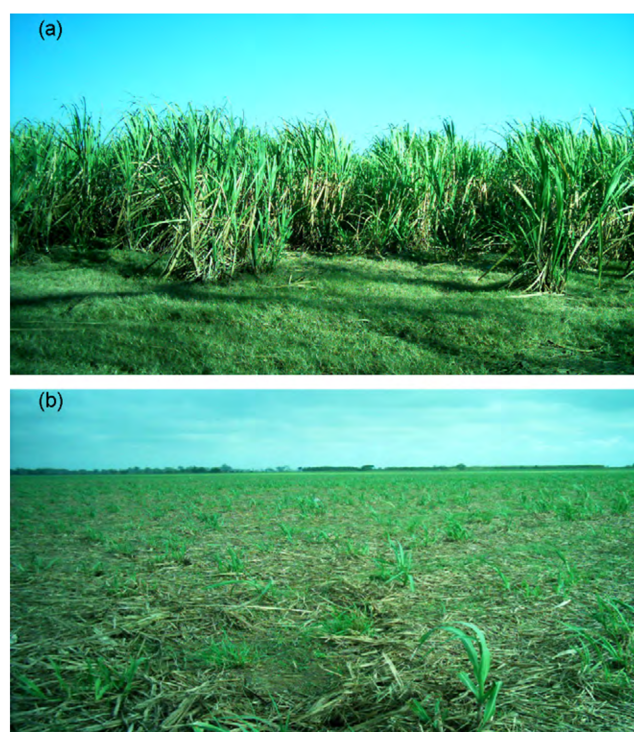

Fig. 2. Photographs of the studied sugarcane field: (a) before harvest and (b) after harvest.

significant deviation from the normal distribution) were performed on soil penetrometer resistance distributions. Those data normality analyses were conducted using STATISTICA™ Software Package (Stat Soft, 2003).

We searched for both isotropic and/or anisotropic prefractal semivariograms using GS + Geostatistics Software Package (Gamma Design Software, 2001). This software uses Eqs. (4) and (5) for computing D_v values. That is, log–log plots of $\gamma(h)$ versus h allow one to estimate both, D_v from the slope of the regression line and the scaling (nugget) coefficient, c, from the $\gamma(h)$-axis intercept. Before sugarcane harvest (12×12 points grid) we considered 124.45 m as the active lag distance and 12.45 m as the lag class distance interval (uniform interval). After crop harvest (10×10 points grid) we chose 101.82 m as the active lag distance and 10.18 m as the lag class distance interval (uniform interval). North direction was selected as the principal axis orientation while offset tolerance was fixed to 22.5°. All of them were software default parameters.

4. Results and discussion

4.1. Description of penetrometer resistance data

Table 2 shows the descriptive statistics of soil penetrometer resistance in the field. Minimum, maximum and mean values increased with soil depth before and after sugarcane harvest but the largest estimates were found after crop harvest. At the same time it was found that there was significant spatial variability in terms of the coefficient of variations. The Shapiro–Wilk test of normality showed that four out of eight samples did not differ statistically from the normal distribution (Figs. 3 and 4). Furthermore, neither log-normal nor gamma distributions yielded significant fits for those non-Gaussian experimental data. A similar situation was found after square-root transformations. There was found a controversial result for a particular data set. For example, while the Kolmogorov–Smirnov test identified a sample as normal, both the Shapiro–Wilk test and Lilliefors probabilities classified

Table 2
Standard descriptive statistics of soil penetration resistance.

Soil depth (cm)	Mean (MPa)	Min. (MPa)	Max. (MPa)	CV (%)	Distribution[a]
Before harvest					
0–2.5	0.550	0.075	3.930	145	Non-Gaussian
2.5–5.0	1.536	0.080	4.250	67	Non-Gaussian
5.0–7.5	2.361	0.180	4.700	35.5	Gaussian
7.5–10.0	2.706	0.350	6.040	31.2	Gaussian
After harvest					
0–2.5	1.163	0.085	5.930	114	Non-Gaussian
2.5–5.0	2.164	0.110	6.460	69	Non-Gaussian
5.0–7.5	2.906	0.140	6.490	52	Gaussian
7.5–10.0	3.160	0.090	6.490	45	Gaussian

[a] After a Shapiro–Wilk test of normality ($p < 0.05$). $n = 144$ data points before harvest and $n = 100$ measurements after harvest.

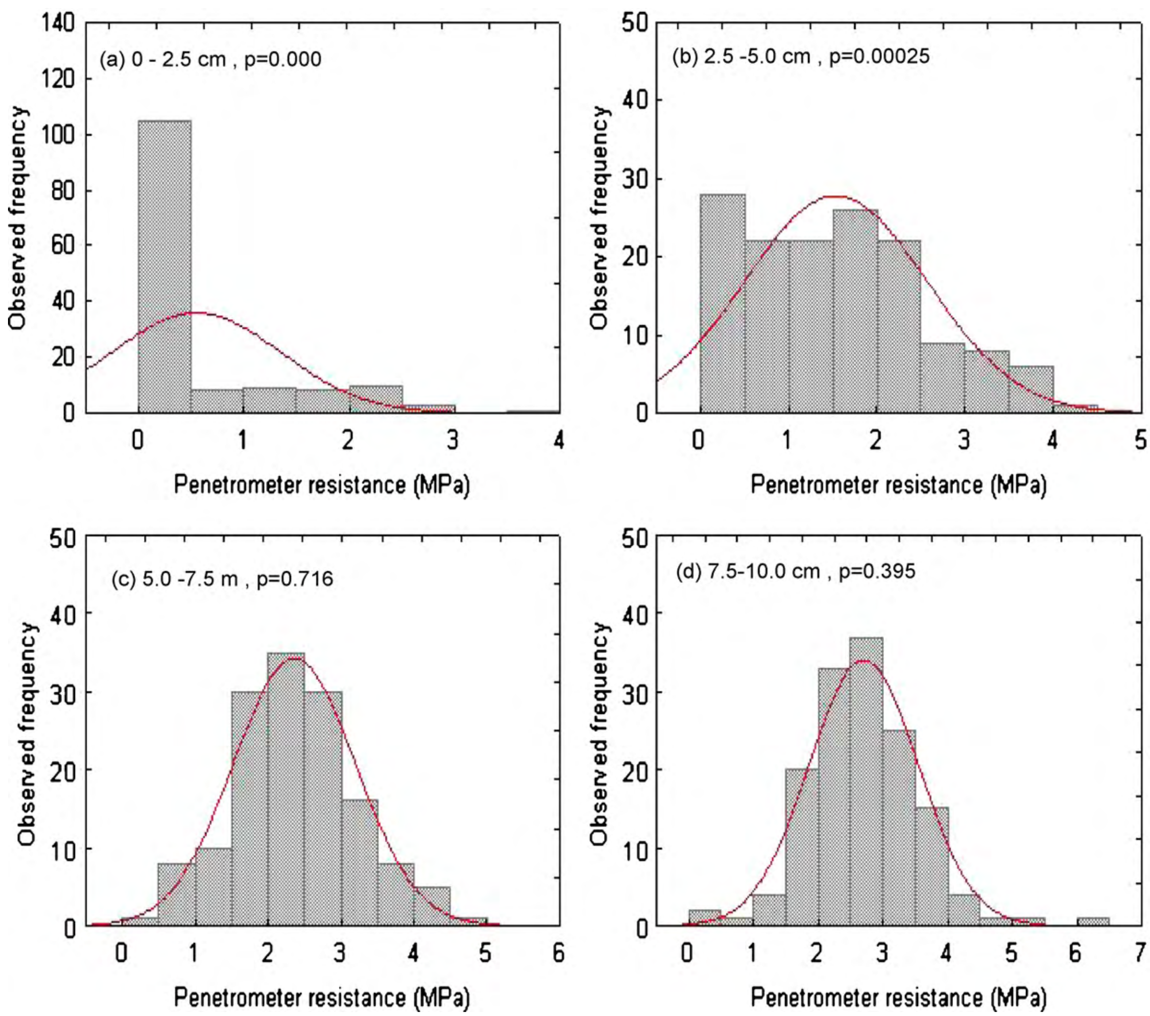

Fig. 3. Histograms of the measured penetrometer resistance before sugarcane harvest (p refers to the Shapiro–Wilk significance level and the continuous curve is the expected normal fit).

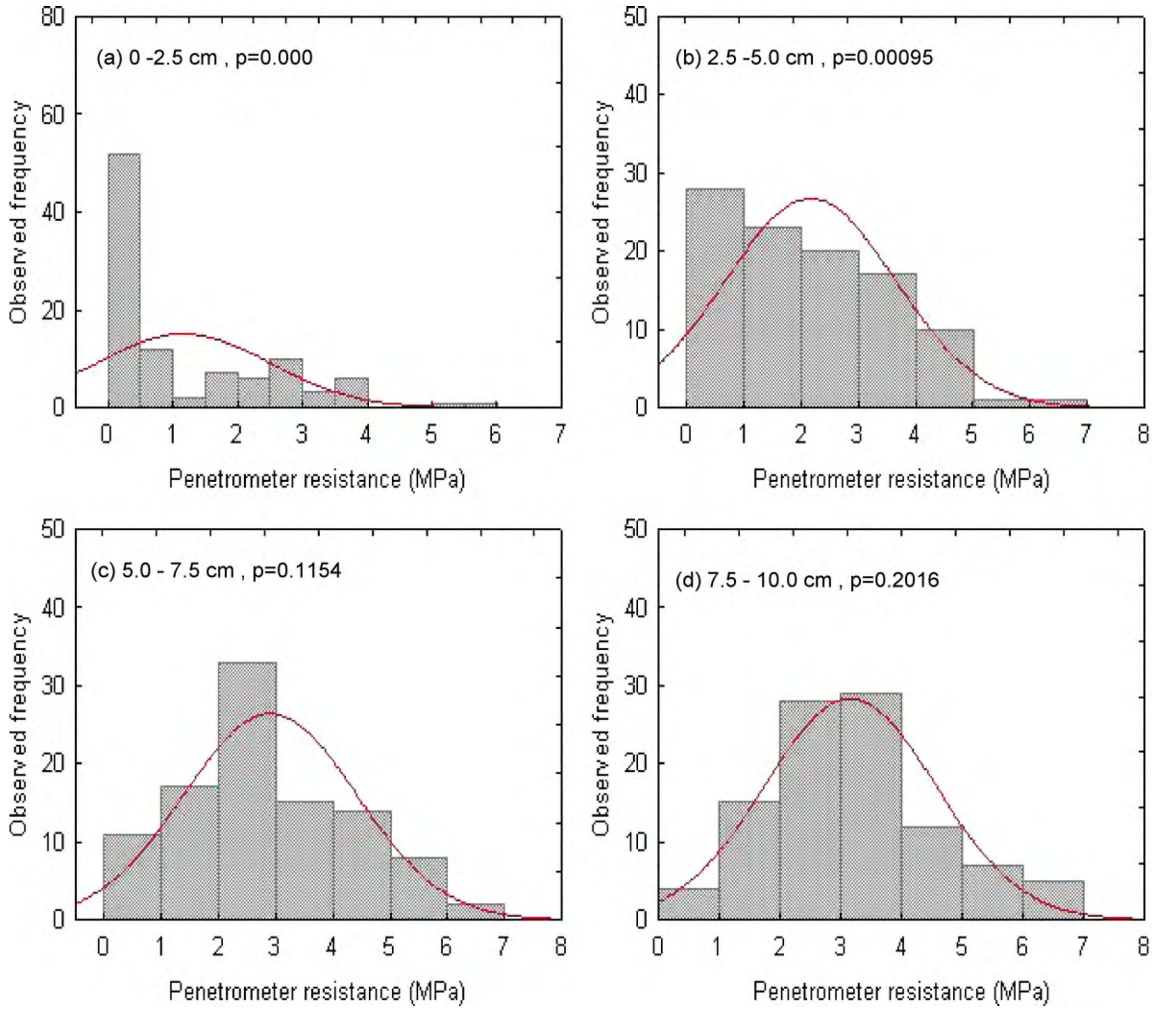

Fig. 4. Histograms of the measured penetrometer resistance after sugarcane harvest (p refers to the Shapiro–Wilk significance level and the continuous curve is the expected normal fit).

that distribution as non-Gaussian (see Fig. 4(b)). We also found that Pareto distributions fitted quite well those frequency (probability) distributions shown in Fig. 3(a) and Fig. 4(a) with coefficient of determinations $R^2 = 0.992$ ($p < 0.01$) and $R^2 = 0.941$ ($p < 0.05$), respectively.

The soil was slightly wetter before sugarcane harvest (February/2009) due to moderately rainy days previous to soil sampling and data collection (Table 3). We think however that soil moisture differences shown in Table 3 do not influence penetrometer resistance interpretations. Figs. 5 and 6 show the spatial distribution of soil penetrometer resistance before and after sugarcane harvesting, respectively. In both cases each data distribution was previously converted into a regular *XYZ* matrix (*Z* representing soil penetration resistance data). In this case crop inter-rows and machinery paths are oriented in the North direction. Both figures are linked to Table 4. As different authors have stated different extreme values for soil compaction (0% of root elongation rate), we used 2.5 MPa as a threshold for separating compacted from uncompacted soil. One can note the dominance of cone index values smaller than 2 MPa before harvest for 0–2.5 cm soil depth (Fig. 5(a)). It is also evident from Table 4 and Figs. 5 and 6 that percentage of mechanical impedance values $\geq$2.5 MPa increased with soil depth in both situations. However, after crop harvest the total percentage of penetrometer resistance data $\geq$2.5 MPa was 47.5% as compared to only 30% before the traffic of harvesting machinery. One can also note from Fig. 6 different spatial patterns of soil penetrometer resistance values as compared to those presented in Fig. 5. Furthermore, inspection of both figures reveals some sort of spatial organization except for Fig. 5b and Fig. 6b) where the spatial structures seem to be random-like fields.

Table 3
Soil gravimetric water content (0–10 cm soil depth).

Before harvest	Values	After harvest	Values
Mean (kg kg^{-1})	0.167	Mean (kg kg^{-1})	0.150
Min. (kg kg^{-1})	0.105	Min. (kg kg^{-1})	0.077
Max. (kg kg^{-1})	0.294	Max. (kg kg^{-1})	0.205
CV (%)	25.88	CV (%)	17.38

$n = 15$ soil samples in each case.

4.2. Spatial prefractal patterns of soil penetrometer resistance distributions

Figs. 7 and 8 present the statistical fit of log–log transformations of Eq. (4) with experimental semivariograms (offsets = 0, 45, 90 and 135 degrees). All the fits were significant ($p < 0.05$) (Table 5), with prefractal scaling exponents ranging from $D_\nu = 1.794$ to $D_\nu = 1.945$ which correspond to anti-persistent patterns. There was an unclear trend of scaling exponent (D_ν) values with soil depth before and after crop harvest. However, before crop harvest the prefractal pattern was isotropic at 0–2.5 cm soil depth. After sugarcane harvest that spatial structure was broken and it turned

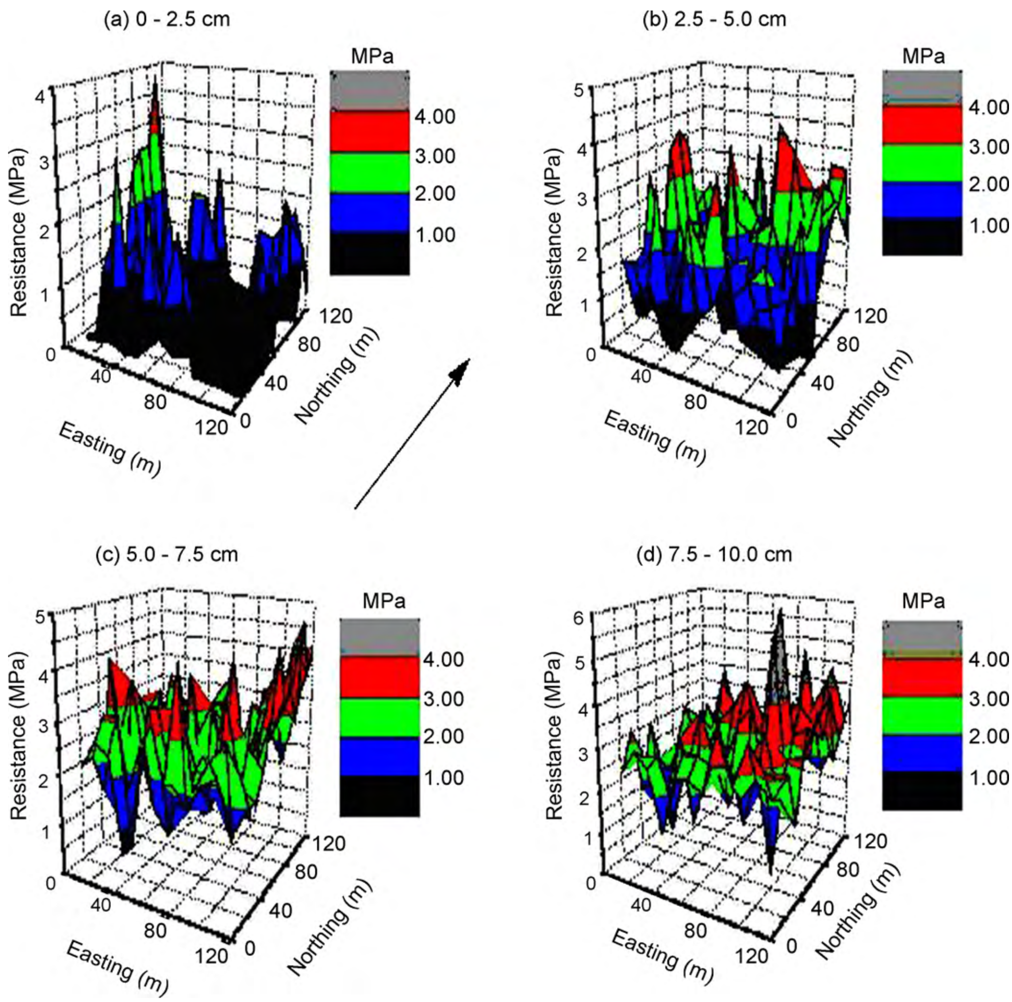

Fig. 5. Spatial distribution of soil impedance data before harvest (the arrow indicates direction of machinery path).

out to be an anisotropic prefractal structure with a prefractal dimension smaller than its isotropic counterpart. In that case the anisotropic prefractal pattern was oriented along the *x*-axis (east direction). Thus, sugarcane harvester and complementary trucks, trailers and tractors induced an anisotropic, anti-persistent prefractal pattern on the 0–2.5 cm soil layer which implies short-range spatial variations of soil penetrometer resistance. In general, there is few information on the application of fractal analysis with spatial data collected from squared grids or other two-dimensional sampling schemes. In a recent paper, Usowicz and Lipiec (2009) reported fractal dimensions computed from isotropic semivariograms of soil impedance data. However, those authors discussed the presence of anisotropic patterns of penetration resistance in terms of vertical and horizontal soil sampling planes.

Regarding 2.5–5.0 cm soil layer, no prefractal structures were found (Table 5). In addition, standard geostatistical models (e.g. linear, exponential, spherical or Gaussian) based on data normality (the intrinsic hypothesis of Geostatistics) did not fit the data significantly (results not shown). In both cases (before and after crop harvest) semivariance values remained almost constant with no dependence on the spatial lag (pure nugget) which is typical of random variations. There were also found different anisotropic prefractal patterns for 5.0–7.5 cm soil depth (45° and 90° directions, respectively). The prefractal dimension value ranged from $D_v = 1.794$ before crop harvest to $D_v = 1.925$ after sugarcane harvest, indicating an increase in the degree of anti-persistence. Similar anisotropic structures were found for 7.5–10.0 cm soil layer, but in this case the semivariogram dimension decreased from $D_v = 1.931$ before harvest to $D_v = 1.870$ after harvest, indicating a slight reduction of the anti-persistence. In general, D_v values > 1.5 suggest that successive soil penetration resistance values are negatively correlated. Cassel and Edwards (2003) associated those short-range variations to bulk density variability due to wheel and machinery compaction so as differences in spatial geometry of previous tillage operations. One can note, however, that nugget semivariances were quite different before crop harvesting (e.g. 0.524, 0.363 and 0.588 MPa^2 for 0–2.5, 5.0–7.5 and 7.5–10.0 cm soil depths, respectively) as compared to those values after sugarcane harvesting (e.g. 1.122, 1.698 and 1.349 MPa^2 for 0–2.5, 5.0–7.5 and 7.5–10.0 cm soil depths, respectively) (Figs. 7 and 8). This suggests that not only fractal dimensions are important for describing scale dependence but also prefractal coefficients are also useful to gain additional information. For instance, the prefractal nugget (*c* in Eq. (4)) conveys information on the amplitude of the variability at the minimal spatial scale ($h = 1$) and the way that spatial pattern is magnified when *h* increases.

From our point of view, persistence/anti-persistence concepts are better illustrated by making use of the original idea suggested in Mandelbrot and Wallis (1969). One approximates the first derivative as a first-order finite difference in Eq. (4) (e.g. $\Delta\gamma(h)/\Delta h$)), to compute the rate of change of the semivariance as a function of the spatial lag, *h*. We used this approach following the rationale proposed by Feder (1988) for analyzing the anomalous diffusivity in fractal media. Then one can plot $\Delta\gamma(h)/\Delta h$ versus *h*

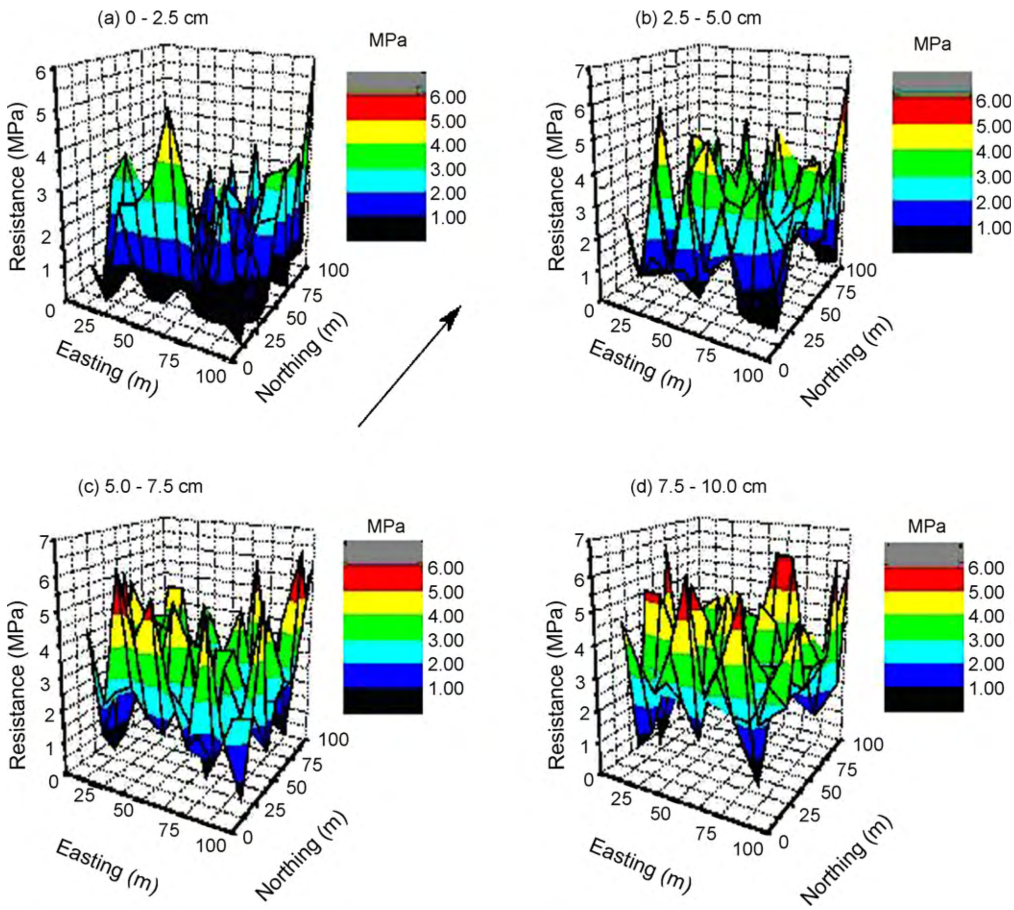

Fig. 6. Spatial distribution of soil impedance data after harvest (the arrow indicates direction of machinery path).

(note that $2H = 4 - 2D_v$). Fig. 9 shows the plots for untransformed coordinates (Fig. 9(a)) and log–log coordinates (Fig. 9(b)), respectively. For the sake of simplicity we set $(1/2)c = 1$ in Eq. (4). For $H = 0.7$ ($D_v = 1.3 < 1.5$) one can note that larger values of semivariance increments are also followed by larger ones as the spatial lag increases. This is the case of persistence. On the other hand, larger values of semivariance increments are followed by smaller ones for $H = 0.3$ ($D_v = 1.7 > 1.5$). This is the case of anti-persistence. Furthermore, note that the magnitude of the semivariance change is not the same for both cases. For example, $\Delta\gamma(h) = +0.325$ between the lags $h = 2$ and $h = 3$ for $H = 0.7$, while $\Delta\gamma(h) = -0.068$ between the same spatial lags for $H = 0.3$. All of this shed light, to some extent, on the spatial scaling of soil penetrometer resistance as a function of the spatial direction. Finally, the case $H = 0.5$ ($D_v = 1.5$) corresponds to uncorrelated values between semivariance rate and spatial lag. With illustrative proposal, we simulated two-dimensional random fields of isotropic fractional Brownian motions for $H = 0.3$, $H = 0.5$ and $H = 0.7$ as shown in Fig. 10(a–c) ($n = 250$). Our hypothetical variable (e.g. soil resistance values) is represented by random increments $0 < \Re \leq 1$.

Table 4
Percentage of soil resistance values $\geq$2.5 MPa.

Soil depth (cm)	Before harvest (%)	After harvest (%)
0–2.5	4.2	21
2.5–5.0	16.7	42
5.0–7.5	41.7	59
7.5–10.0	57.6	68
Total	30.0	47.5

$n = 144$ data points before harvest and $n = 100$ measurements after harvest.

All the simulated fields were synthesized using FracLab Software (Institut National de Recherche en Informatique et Automatique, 1998). The anti-persistent case ($H = 0.3$, Fig. 10(a)) presents short-range fluctuations similar, to some extent, to white noise.

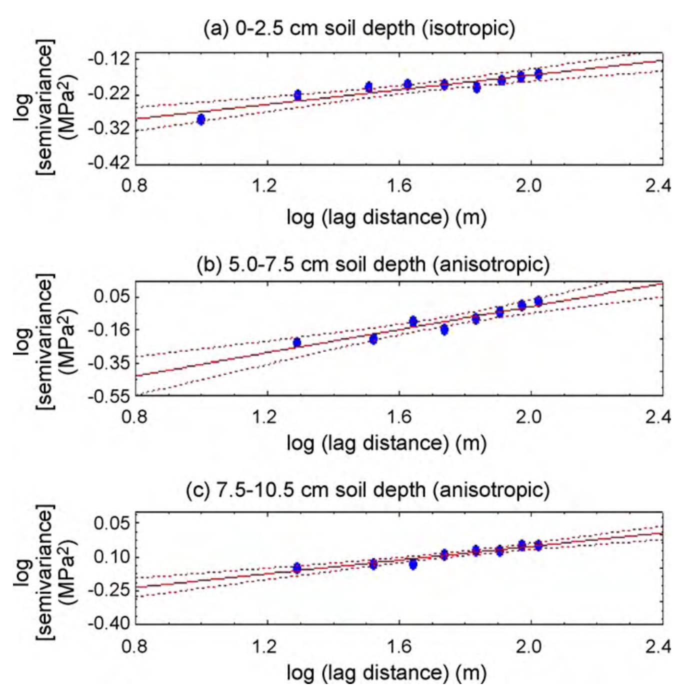

Fig. 7. Log–log plot of the geostatistical prefractal model before sugarcane harvest.

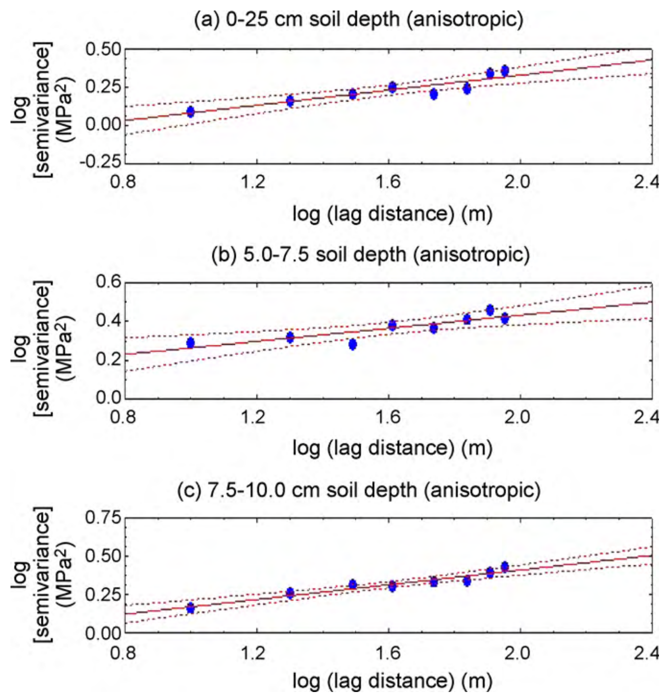

Fig. 8. Log–log plot of the geostatistical prefractal model after sugarcane harvest.

However, one can note smaller values followed by larger ones and vice versa (see scale bar at the right hand of each figure). The white noise (regular Brownian motion) simulation ($H = 0.5$, Fig. 10(b)) does not show a well defined structure as expected. On the other

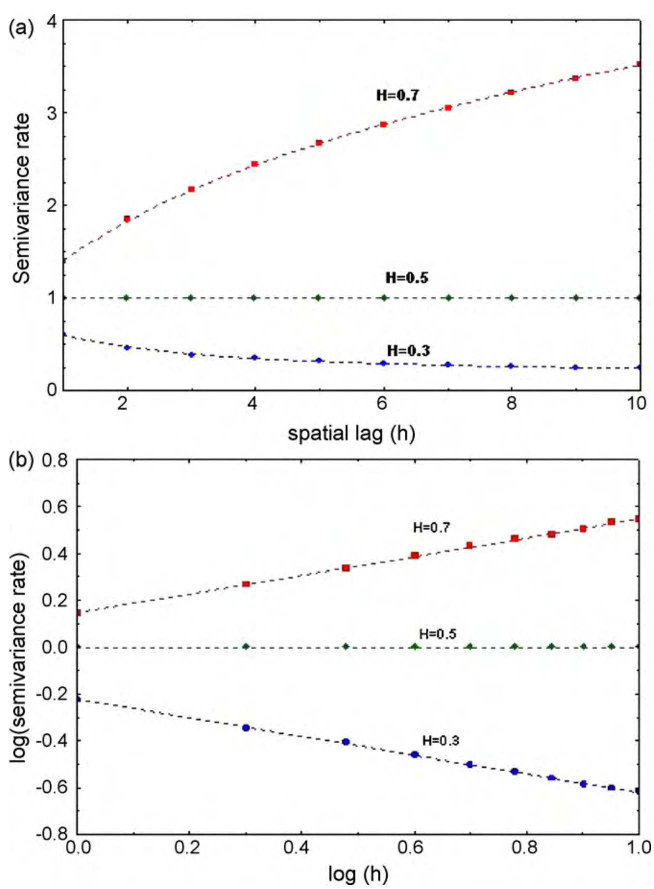

Fig. 9. Semivariance rate of variation as a function of the spatial lag: (a) untransformed coordinates and (b) log–log representation.

Table 5
Prefractal patterns before and after crop harvest (offset tolerance = 22.5°).

Soil depth (cm)					Soil depth (cm)				
Before harvest	Model	Offset (°)	D_v (±std)	R^a	After harvest	Model	Offset (°)	D_v (±std)	R^a
0–2.5	Isotropic	–	1.945 (0.015)	0.941	0–2.5	Anisotropic	90	1.875 (0.05)	0.938
2.5–5.0	No structure[b]	–	–	–	2.5–5.0	No structure[b]	–	–	–
5.0–7.5	Anisotropic	45	1.794 (0.05)	0.955	5.0–7.5	Anisotropic	90	1.925 (0.03)	0.911
7.5–10.0	Anisotropic	45	1.931 (0.017)	0.981	7.5–10.0	Anisotropic	90	1.870 (0.05)	0.963

[a] R refers to the correlation coefficient ($p < 0.05$).
[b] No prefractal structure.

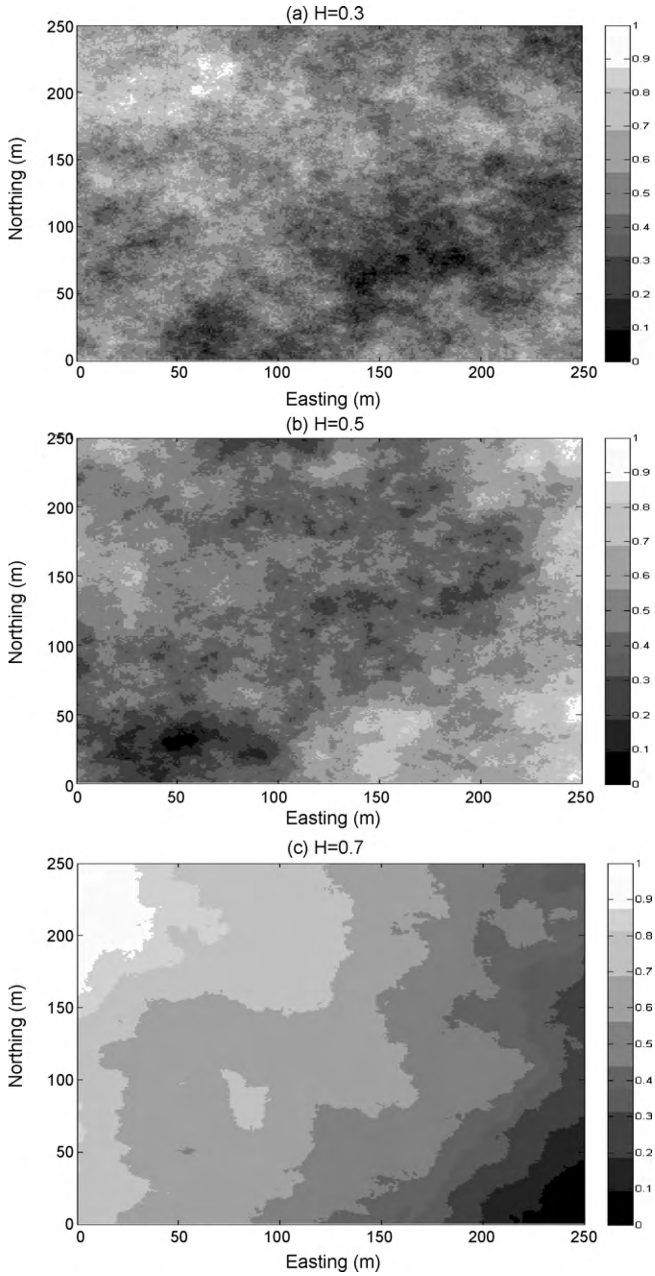

Fig. 10. Two-dimensional random fields synthesizing fractional Brownian motions: (a) anti-persistence, (b) white noise and (c) persistence.

hand, the positively correlated pattern (H = 0.7, Fig. 10(c)) shows large zones with a persistent range of values. In general, harvesting machinery can change, in many cases, the spatial organization and orientation of soil compaction zones. Furthermore, soil dynamics, in terms of soil mechanical properties, can change their spatial scaling in response to harvesting machinery. Even though soil resistance was measured at inter-row, the transient strain is transmitted both downward and laterally which also influences crop root system (Cassel and Edwards, 2003). Or and Ghezzehei (2002) have pointed out that both, plastic and elastic deformations can occur within 10 cm below the soil surface. We also include the spatial re-organization of both, normal and tangential (shearing) stresses which determine, to a large extent, soil penetrometer resistance. This type of complex organization influences other physical properties of the soil. For example, one could expect similar prefractal scaling patterns of soil structure degradation in terms of increasing bulk density values. In general, that is not a very serious problem with Vertisols as natural shrinking/swelling processes tend to restore the original soil structure. However, some crop dependent parameters such as rate of shoot emergence and roots distribution might be affected as previously pointed out.

5. Conclusions

We have used classical statistics, prefractal analysis and approximations to Pareto-type behavior with soil penetrometer resistance data before and after sugarcane harvest in order to characterize soil plow layer penetrometer resistance under mechanized sugar cane production. The Shapiro–Wilk test of normality showed that four out of eight distributions were normal within the considered spatial scale. The experimental semivariance increased as a function of the spatial lag following a prefractal (Pareto-type) law in most cases. In addition to increasing soil compaction, harvesting machinery produced changes on the anisotropic direction of prefractal patterns. All the prefractal structures rendered scaling parameters larger than 1.5 indicating anti-persistence, short-range variations of soil penetrometer resistance and anti-correlation. This type of prefractal spatial variation can account for differences of sugarcane yield within the field. In general, the combination of Geostatistics and prefractal analysis can assist the mechanized agriculture and scientists through a previous identification of degraded zones within the field (e.g. block kriging) and the physical processes involved in the formation of those local areas (e.g. prefractal statistics). With this information, the agricultural supervisor can manage the cultivation of sugarcane fields in order to minimize or remediate areas of physically degraded soil, and to increase production yields.

Acknowledgments

We appreciate the valuable critical comments and suggestions by the Editor and reviewers which help us to improve the quality of the original manuscript.

References

Armstrong, A.C., 1986. On the fractal dimensions of some transient soil properties. J. Soil Sci. 37, 641–652.

Baveye, P., Boast, C.W., Gaspard, S., Tarquis, A.M., Millán, H., 2008. Introduction to fractal geometry, fragmentation processes and multifractal measures: theory and operational aspects of their application to natural systems. In: Senesi, N., Wilkinson, K.J. (Eds.), Biophysical Chemistry of Fractal Structures and Processes in Environmental Systems. IUPAC Series on Analytical and Physical Chemistry of Environmental Systems, vol. 11. John Wiley and Sons, Chichester, UK, pp. 11–67.

Burrough, P.A., 1989. Fractals and geochemistry. In: Avnir, D. (Ed.), The Fractal Approach to Heterogeneous Chemistry. John Wiley and Sons, Chichester, UK, pp. 383–406.

Cassel, D.K., Edwards, E.C., 2003. Scaling soil mechanical properties to predict plant responses. In: Pachepsky, Ya., Radcliffe, D.E., Selim, H.M. (Eds.), Scaling Methods in Soil Physics. CRC Press, Boca Raton, FL, pp. 279–294.

Duiker, S.J., 2002. Diagnosing soil Compaction Using a Penetrometer (Soil Compaction Tester). Agronomy Facts 63. Publications Distribution Center, The Pennsylvania State University, PA, pp. 4.

Feder, J., 1988. Fractals. Plenum Press, New York, NY.

Gamma Design Software, 2001. GS+ Geostatistics for the Environmental Sciences, version 5.1.1, Professional Edition. Plainwell, MI.

Gee, G.W., Bauder, J.W., 1986. Particle size analysis. In: Klute, A. (Ed.), Methods of Soil Analysis. 2nd edition. ASA, Madison, WI, pp. 383–411.

Hadas, A., 1997. Soil tilth-the desired soil structural state obtained through proper soil fragmentation and reorientation processes. Soil Tillage Res. 43, 7–40.

Hartemink, A.E., 1998. Soil chemical and physical properties as indicators of sustainable land management under sugar cane in Papua New Guinea. Geoderma 85, 283–306.

Institut National de Recherche en Informatique et Automatique (INRIA), 1998. FracLab 2.04. A fractal analysis toolbox for signal and image processing. http://fraclab.saclay.inria.fr.

Juang, T.C., Uehara, G., 1971. Effects of ground-water table and soil compaction on nutrient element uptake and growth of sugarcane. Int. Soc. Sugarcane Technol. 14, 679–687.

Keller, T., 2004. Soil compaction and soil tillage studies in agricultural soil mechanics. Ph.D. Dissertation, Swedish University of Agricultural Sciences, Uppsala.
Kiliç, K., Özgöz, E., Akbą, F., 2000. Assessment of spatial variability in penetration resistance as related to some soil physical properties of two fluvents in Turkey. Soil Tillage Res. 76, 1–11.
Korvin, G., 1992. Fractal models in the Earth Sciences. Elsevier, Amsterdam.
Krasilnikov, P., 2008. Variography of discrete soil properties. In: Krasilnikov, P., Carré, F., Montanarella, L. (Eds.), Soil Geography and Geostatistics. Concepts and Applications. JRC Scientific and Technical Reports, Chapter 2. Office for Official Publications of the European Communities, Luxembourg, pp. 12–25.
Mandelbrot, B.B., 1985. Self-affinity and fractal dimension. Phys. Scripta 32, 425–436.
Mandelbrot, B.B., 1986. Self-affine fractal sets: the basic fractal dimension. In: Pietronero, L., Tosatti, E. (Eds.), Fractals in Physics. North Holland, Amsterdam.
Mandelbrot, B., Wallis, J.R., 1969. Computer experiments with fractional Gaussian noises. Part 1. Sample graphs, averages and variances. Water Resour. Res. 5, 283–305 (H12).
Materechera, S.A., Dexter, A.R., Alston, A.M., 1991. Penetration of very strong soils by seedling roots of different plan species. Plant Soil 135, 31–34.
Matheron, G., 1971. The Theory of Regionalized Variables and Its Applications. Les cahiers du centre de morphologic mathematique de Fontainebleau, Paris, ENSMP, Fasc. no. 5.
McClean, C.J., Evans, I.S., 2000. Apparent fractal dimensions from continental scale digital elevation models using variogram methods. Trans. GIS 4, 361–378.
Molz, F.J., Hewett, T.A., Boman, G.K., 1998. A pseudo-fractal model for hydraulic property distributions in porous media. In: Baveye, P., Parlange, J.-Y., Stewardt, B.A. (Eds.), Advances in Soil Science. Fractals in Soil Science. CRC Press, Boca Raton, FL, pp. 341–372.
Or, D., Ghezzehei, T.A., 2002. Modeling post-tillage soil structural dynamics: a review. Soil Tillage Res. 64, 41–59.
Pan, J., Lu, Z., 1994. Fractal dimensions of soil strengths for paddy fields in China. J. Terramech. 31, 1–9.
Perfect, E., Díaz-Zorita, M., Grove, J.H., 2002. A prefractal model for predicting soil fragment mass-size distributions. Soil Tillage Res. 64, 79–90.
Perfect, E., Groenevelt, P.H., Kay, B.D., Grant, C.D., 1990. Spatial variability of soil penetrometer measurements at the mesoscopic scale. Soil Tillage Res. 16, 257–271.
Soil Survey Staff, 2003. Keys to Soil Taxonomy, 9th edition. USDA-NRCS, Washington, DC, pp. 332.
Stat Soft, Inc., 2003. STATISTICA (Data Analysis Software System), version 6. Tulsa, OK.
Sugarcane Production BMPs, 2000. Sugarcane Production Best Management Practices Report. Louisiana State University Agricultural Center, pp. 40.
Thomas, T.R., Thomas, A.P., 1988. Fractals and engineering surface roughness. Surf. Topogr. 1, 143–152.
Turcotte, D.L., 1997. Fractals and Chaos in Geology and Geophysics, 2nd edition. Cambridge University Press.
Usowicz, B., Lipiec, J., 2009. Spatial distribution of soil penetration resistance as affected by soil compaction: the fractal approach. Ecol. Complex. 6, 263–271.
Webster, R., 2008. Soil science and geostatistics. In: Krasilnikov, P., Carré, F., Montanarella, L. (Eds.), Soil Geography and Geostatistics. Concepts and Applications. JRC Scientific and Technical Reports, Chapter 1. Office for Official Publications of the European Communities, Luxembourg, pp. 1–11.
Webster, R., Burgess, T.M., 1980. Optimal interpolation and isarithmic mapping of soil properties: changing drift and universal kriging. J. Soil Sci. 31, 505–524.
Webster, R., Oliver, M.A., 1992. Sample adequately to estimate variograms of soil properties. J. Soil Sci. 43, 177–192.
Wu, J.-J., 2000. Characterization of fractal surfaces. Wear 239, 36–47.